

Single-Electron Charge Transfer and Excitations at Collisions between Bi^{4+} Ions in the Kiloelectronvolt Energy Range

V. K. Nikulin and N. A. Guschina

*Ioffe Physicotechnical Institute, Russian Academy of Sciences,
Politekhnicheskaya ul. 26, St. Petersburg, 194021 Russia*

e-mail: nikulin@astro.ioffe.ru

Received July 6, 2006

Abstract—Pioneering theoretical data for single-electron charge transfer and excitations due to collisions between Bi^{4+} ions in the ground ($6s$) and metastable ($6p$) states are gained in the collision energy interval 5–75 keV in the center-of-mass frame. The cross sections of the processes are calculated in terms of the close-coupling method in the basis of two-electron quasi-molecular states for the Coulomb trajectory of nuclei. It is found that single-electron capture into the singlet $6s^2$ states of Bi^{3+} ions makes a major contribution to the charge transfer total cross section for $\text{Bi}^{4+}(6s) + \text{Bi}^{4+}(6s)$ collisions (reaction 1), whereas single-electron capture into the singlet $6s6p$ states is the basic contributor to the total cross section in $\text{Bi}^{4+}(6s) + \text{Bi}^{4+}(6p)$ collisions (reaction 2). In the collision energy interval mentioned above, the collision cross sections vary between 1.2×10^{-17} and 1.9×10^{-17} cm² for reaction 1 and between 3.8×10^{-17} and 5.3×10^{-17} cm² for reaction 2. In reaction 1, the $6s \rightarrow 6p$ excitation cross sections vary from 0.6×10^{-16} to 0.8×10^{-16} cm² for the singlet channel and from 2.2×10^{-16} to 2.8×10^{-16} cm² for the triplet channel. The calculation results are compared with the data obtained in experiments with crossed ion beams of kiloelectronvolt energy. The fraction of metastable ions in the beams is estimated by comparing the experimental data with the weighted average theoretical results for the cross sections of reactions 1 and 2. From the data for the charge transfer cross sections, one can estimate particle losses in relativistic beams due to a change in the charge state of the ions colliding with each other in the beam because of betatron oscillations.

PACS numbers: 34.70.+e, 34.10.+x

DOI: 10.1134/S1063784207020028

INTRODUCTION

Collisions between multiply charged heavy ions have been little studied theoretically in the physics of atomic collisions. Gaining insight into charge transfer between identical low-charged heavy ions is vital to designing accelerators and storage rings with the aim to generate intense ion beams. Such beams can also find application in heavy-ion-driven inertial fusion [1]. When generating intense beams, one should estimate particle losses in the beams because of a change in the charge state of ions (due to charge transfer and ionization) colliding in the beam. Charge transfer in the beam takes place at a collision energy of ions of ≈ 50 keV in the center-of-mass frame when they move normally to the beam direction because of betatron oscillations.

Recently, the charge transfer total cross sections were measured in slow collisions between four-charged Ar, Kr, Xe, Pb, and Bi heavy ions in experiments with crossed beams [2]. The results obtained in [2] are to an

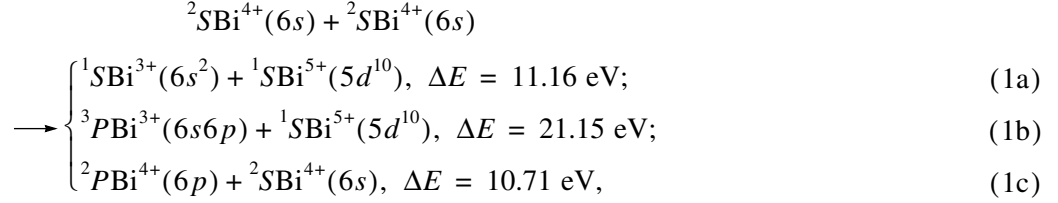
extent uncertain, since the crossed beam had metastable ions, for which the cross section of collision-induced charge transfer is larger than for ions in the ground state. Additional experiments showed [2] that the fraction of metastable ions amounts to 12–29% for Ar^{4+} , Kr^{4+} , and Xe^{4+} ions. For these ions, the ionization cross sections were also measured and the particle losses in the beam were estimated [2].

In this work, we give a theoretical analysis of the charge transfer and excitation processes occurring in collisions between Bi^{4+} ions in the ground ($6s$) and metastable ($6p$) states.

The fraction of metastable ions in the beam is estimated by comparing the calculated and experimental results for the charge transfer total cross sections.

We consider the processes of single-electron charge transfer (reactions 1a and 1b, see below) and excitation (process 1c) taking place in collisions between Bi^{4+}

ions in the ground state for the singlet and triplet reaction channels,

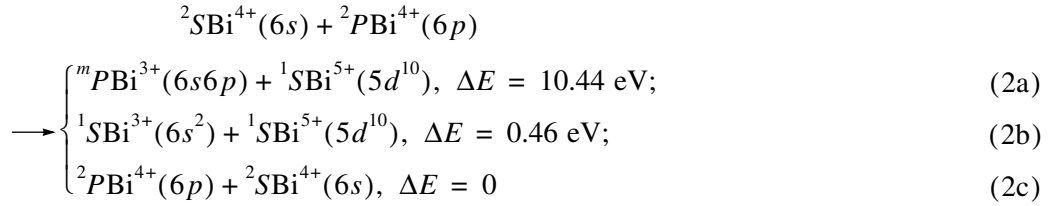


where ΔE is the resonance defect.

The singlet and triplet entrance channels were also considered for excitations (1c).

For the triplet channel of single-electron charge transfer, the resonance defect is much higher than for the singlet channel. Therefore, channel (1b), as well as

collisions between ions in the ground and metastable states, was ignored in our earlier publication [3]. Here, we consider the singlet ($m = 1$) and triplet ($m = 3$) channels of charge transfer reactions taking place in collisions between ions in the ground and metastable states,



(reaction (2c) was considered for both the singlet and triplet entrance channel).

The ion total energy used to estimate the resonance defects was calculated in the relativistic Hartree–Fock–Slater approximation.

THEORETICAL GROUNDS

The cross sections of reactions 1 and 2 were calculated in a quasi-classical approximation in terms of the close-coupling method in the basis of two-electron quasi-molecular states (the effect of electrons of $\text{Bi}^{5+}(5d^{10})$ ion cores was taken into account by the effective potential technique). In this approximation, the problem reduces to finding electron wave function $\tilde{\Psi}(r_1, r_2, t)$ that satisfies the nonstationary Schrödinger equation

$$i \frac{\partial \tilde{\Psi}(r_1, r_2, t)}{\partial t} = H(r_1, r_2, R(t)) \tilde{\Psi}(r_1, r_2, t), \quad (3)$$

where $H(r_1, r_2, R(t))$ is the two-electron Hamiltonian, which parametrically depends on time through nuclear spacing $R(t)$,

$$H = \sum_{k=1,2} H_0(r_k; R) + \frac{1}{r_{12}}. \quad (4)$$

Here, $H_0(r_k; R)$ is specified for each one-electron

molecular orbital $\psi_n(r_k; R)$ in the form

$$H_0(r_k; R) = -\frac{\nabla_k^2}{2} + V_{\text{eff}}^2(r_k; R). \quad (5)$$

Effective potential $V_{\text{eff}}^2(r_k; R)$ taking into account that the quasi-molecule contains many electrons is specified parametrically [4],

$$\begin{aligned}
 V_{\text{eff}}^n(r_k; R) = & -\frac{Z_A}{r_{ak}} - \frac{Z_B}{r_{bk}} + \frac{1}{2} \left[\frac{a_1^n - b_1^n}{r_{ak}} + \frac{a_1^n + b_1^n}{r_{bk}} \right. \\
 & \left. + \frac{\tilde{a}_1^n + R a_0^n}{r_{ak} r_{bk}} + \frac{b_2^n (r_{ak} - r_{bk})^2}{R r_{ak} r_{bk}} \right]. \quad (6)
 \end{aligned}$$

In (3)–(6), r_k are the coordinates of outer-shell electrons, r_{ak} and r_{bk} are the distances of a k th electron to nuclei with charges Z_A and Z_B (A is an incident ion, and B is the target; $Z_A = Z_B = 5$), and r_{12} is the distance between the electrons. The effective potential in form (6) allows separation of variables in the one-electron Schrödinger equation,

$$H_0(r; R) \psi_n(r; R) = \varepsilon_n(R) \psi_n(r; R) \quad (7)$$

in the prolate spheroidal coordinate system. This, in turn, makes it possible to obtain [4] diabatic screened diatomic molecular orbitals (SDMOs) ψ_n that preserve the symmetry of commonly used one-electron diatomic molecular orbitals of H_2^+ [5]. Parametrization of the effective potential is discussed below. SDMOs are categorized based on the spherical quantum numbers (n, l ,

m) of the state of a united atom into which a given orbital passes at $R \rightarrow 0$. A correspondence between a given orbital and atomic levels at $R \rightarrow 0$ and $R \rightarrow \infty$ is established using the Barat–Lichten correlation rules [6].

A solution to Eq. (3) is sought in the form of expansion in orthonormalized basis $\Psi_l(r_1, r_2; R)$ of two-electron states,

$$\begin{aligned} \tilde{\Psi}(r_1, r_2, t) = & \sum_{l=1}^n a_l(t) \Psi_l(r_1, r_2; R) \\ & \times \exp\left(-i \int_0^t E_l(R) dt'\right), \end{aligned} \quad (8)$$

where

$$E_l(R) = \langle \Psi_l(r_1, r_2; R) | H | \Psi_l(r_1, r_2; R) \rangle. \quad (9)$$

Substituting (8) into (3) yields a set of linear differential equations in coefficients a_l . For the Coulomb trajectory of nuclei, it has the form [7]

$$\begin{aligned} \frac{da_l(\tau)}{d\tau} = & - \sum_{k \neq l} a_k(\tau) \left\{ \frac{\tau}{R - \gamma} R_{lk}(R) + \frac{\rho}{R(R - \gamma)} L_{lk}(R) \right. \\ & \left. + \frac{i}{v} \frac{R}{R - \gamma} H_{lk}(R) \right\} \exp\left(-i \int_0^\tau (E_k(R) - E_l(R)) \frac{R}{R - \gamma} d\tau\right) \\ & (R(\tau) = (\tau^2 + \gamma^2 + \rho^2)^{1/2} + \gamma; -\infty < \tau < \infty). \end{aligned} \quad (10)$$

Here, ρ is the impact parameter, v is the relative velocity of colliding particles, $\gamma = Z_A Z_B / \mu v^2$, μ is the reduced mass,

$$R_{lk} = \langle \Psi_l(r_1, r_2; R) | d/dR | \Psi_k(r_1, r_2; R) \rangle$$

and

$$L_{lk} = \langle \Psi_l(r_1, r_2; R) | iL_y | \Psi_k(r_1, r_2; R) \rangle \quad (11)$$

are the matrix elements of dynamic (radial, R_{lk} , and rotational, L_{lk}) couplings between the basic states, and

$$H_{lk} = \langle \Psi_l(r_1, r_2; R) | H | \Psi_k(r_1, r_2; R) \rangle \quad (12)$$

Table 1. Parameters of effective potentials V_{eff}^n (in atomic units) used in calculation of SDMOs ψ_n of the $\text{Bi}^{4+} + \text{Bi}^{4+}$ quasi-molecule

Ψ_n	\tilde{a}_1^n	a_1^n	a_0^n	b_2^n
$6s\sigma$	-0.250	-55.94	320.798	-278.863
$7p\sigma$	-2.247	-28.88	141.949	-127.852
$7d\sigma$	-6.110	-5.18	-0.518	-5.832
$8f\sigma$	-10.545	-0.35	-11.267	0.087

are the matrix elements of potential couplings.

When writing close-coupling equation (10) and calculating the dynamic matrix elements, we assumed that the origin of the coordinate system in which the nuclei move is placed in the middle of the nucleus spacing, the z axis coincides with the direction of the incident ion initial velocity, and the y axis runs normally to the plane (xOz) of collision.

To calculate reactions 1 and 2, we took one-electron orbitals

$$\begin{aligned} \psi_1^g = 6s\sigma, \quad \psi_2^u = 7p\sigma, \quad \psi_3^g = 7d\sigma, \\ \psi_4^u = 8f\sigma. \end{aligned} \quad (13)$$

In the separated atom limit, the wave functions of these orbitals are expressed through the even and odd combinations of atomic $6s_A$ and $6s_B$ functions and $6p_A$ and $6p_B$ functions of incident atom A and target atom B ,

$$\begin{aligned} 6s\sigma(r; R)_{R \rightarrow \infty} & \rightarrow \frac{1}{\sqrt{2}}(6s_A + 6s_B), \\ 7p\sigma(r; R)_{R \rightarrow \infty} & \rightarrow \frac{1}{\sqrt{2}}(6s_A - 6s_B), \\ 7d\sigma(r; R)_{R \rightarrow \infty} & \rightarrow \frac{1}{\sqrt{2}}(6p_A + 6p_B), \\ 8f\sigma(r; R)_{R \rightarrow \infty} & \rightarrow \frac{1}{\sqrt{2}}(6p_A - 6p_B). \end{aligned} \quad (14)$$

The parameters of the effective potential used to calculate SDMOs were determined as follows. Quantities \tilde{a}_1^n and a_1^n were found from the requirement that energy $\epsilon_n(R)$ of molecular orbital ψ_n and mean effective potential $\bar{V}_{\text{eff}}^n(r; R) = \langle \psi_n | V_{\text{eff}}^n | \psi_n \rangle$ turn to their respective values $\epsilon_{nl}^{\text{ua}}$ and \bar{V}_{nl}^{ua} obtained by atomic calculations in the united atom limit. Parameters a_0^n and b_2^n (for homonuclear systems, $b_1 \equiv 0$) were determined from the requirement that energy $\epsilon_n(R)$ at large nucleus spacings ($R \rightarrow \infty$) take its asymptotic limit, $\epsilon_n(R)|_{R \rightarrow \infty} \rightarrow \epsilon^{\text{sa}} - 4/R$, where ϵ^{sa} is the energy of an atomic state (n', l', m) into which a given orbital passes in the separated atom limit. Detailed expressions for these parameters are given in [8]. The parameters thus obtained and the values of atomic quantities $\epsilon_{nl}^{\text{ua}}$, \bar{V}_{nl}^{ua} , and ϵ^{sa} are listed in Tables 1 and 2. Orbitals $\psi_n(r; R)$ of the same symmetry that are determined from (7) are nonorthogonal to each other because of the dependence of effective potential V_{eff}^n on state n . The set of orthogonalized [9] one-particle states $\psi_n^l(r; R)$ that corresponds to basic set (13) and is subsequently used to construct an orthogonal

Table 2. Energies $\epsilon_{nl}^{\text{ua}}$ and the mean values of electron potential \bar{V}_{nl}^{ua} for SDMOs ψ_n in the unified atom approximation and energies ϵ^{sa} for SDMOs ψ_n in the separated atom approximation (all the quantities are given in atomic units)

ψ_n	$R = 0$			$R \rightarrow \infty$	
	nl	$\epsilon_{nl}^{\text{ua}}$	\bar{V}_{nl}^{ua}	$n'l'$	ϵ^{sa}
$6s\sigma$	$6s$	-71.637	514	$6s$	-2.004
$7p\sigma$	$7p$	-82.992	663	$6s$	-2.004
$7d\sigma$	$7d$	-4.846	25.9	$6p$	-1.609
$8f\sigma$	$8f$	-1.509	5.39	$6p$	-1.609

basis of two-electron states $\Psi_l(r_1, r_2; R)$ is

$$\begin{aligned} \Psi_1' &\approx \Psi_1^s - \frac{S_{13}}{2} \Psi_3^s, & \Psi_3' &\approx \Psi_3^s - \frac{S_{13}}{2} \Psi_1^s, \\ \Psi_2' &\approx \Psi_2^u - \frac{S_{24}}{2} \Psi_4^u, & \Psi_4' &\approx \Psi_4^u - \frac{S_{24}}{2} \Psi_2^u. \end{aligned} \quad (15)$$

Expressions (15) are written with regard to the smallness of the matrix elements of overlap between orbitals $\psi_n(r; R)$ ($|S_{13}| = |\langle \Psi_1^s | \Psi_3^s \rangle| < 0.17$ and $|S_{24}| = |\langle \Psi_2^u | \Psi_4^u \rangle| < 0.14$). The energies and wave functions of SDMOs, as well as the matrix elements of overlap between them, were calculated using a special program package [10].

Basic two-electron wave functions $\Psi_l(r_1, r_2; R)$ were constructed using symmetrized (even and odd) linear combinations of two-electron one-configuration states $\phi_i(r_1, r_2; R)$ that, in turn, were constructed on orthogo-

nalized one-electron quasi-molecular states $\psi_n'(r_k; R)$,

$$\begin{aligned} \phi_i(r_1, r_2; R) &\equiv \phi_i[\psi_n', \psi_{n'}'] \\ &= \begin{cases} \frac{1}{\sqrt{2}} [\psi_n'(r_1; R) \psi_{n'}'(r_2; R) \pm \psi_{n'}'(r_2; R) \psi_n'(r_1; R)], \\ n \neq n' \\ \psi_n'(r_1; R) \psi_n'(r_2; R), \quad n = n'. \end{cases} \end{aligned} \quad (16)$$

The plus and minus signs appearing in (16) refer to singlet and triplet two-electron states, respectively.

The symmetrized singlet $\Phi_j^{s,u}(r_1, r_2; R)$ and triplet $\bar{\Phi}_j^{s,u}(r_1, r_2; R)$ linear combinations of one-configuration two-electron states $\phi_i(r_1, r_2; R)$ used in calculation of reactions 1 and 2, along with their atomic limits at $R \rightarrow \infty$,

$$\begin{aligned} \chi_j^{s,u}(r_1, r_2) &= \lim_{R \rightarrow \infty} \Phi_j^{s,u}(r_1, r_2; R), \\ \bar{\chi}_j^{s,u}(r_1, r_2) &= \lim_{R \rightarrow \infty} \bar{\Phi}_j^{s,u}(r_1, r_2; R), \end{aligned} \quad (17)$$

obtained using relationships (14), are listed in Tables 3 and 4.

CALCULATION OF SINGLE-ELECTRON CHARGE TRANSFER AND EXCITATIONS IN COLLISIONS BETWEEN GROUND-STATE $\text{Bi}^{4+}(6s)$ ATOMS

Collisions between the ions in the ground state were calculated using five two-electron states $\Psi_l(r_1, r_2; R)$ describing entrance channel Ψ_1 , charge transfer channels Ψ_2 and Ψ_3 (a, a' or b, b'), and channels Ψ_4 and Ψ_5 (c, c') of $6s-6p$ electron excitation in reactions 1. For

Table 3. Symmetrized combinations $\Phi_j^{s,u}(r_1, r_2; R)$ of singlet one-configuration states $\phi_i[\psi_n', \psi_{n'}'] = [\psi_n'(r_1) \psi_{n'}'(r_2) + \psi_{n'}'(r_2) \psi_n'(r_1)] / \sqrt{2}$ and their atomic limits at $R \rightarrow \infty$

$\Phi_j^{s,u}(r_1, r_2; R)$	Limit at $R \rightarrow \infty$ ($\chi_j^{s,u}$)
$\Phi_1^s(r_1, r_2; R) = (\phi_1[\psi_1', \psi_1'] - \phi_2[\psi_2', \psi_2']) / \sqrt{2}$	$[6s_A, 6s_B]$
$\Phi_2^s(r_1, r_2; R) = (\phi_1[\psi_1', \psi_1'] + \phi_2[\psi_2', \psi_2']) / \sqrt{2}$	$(6s_A(1)6s_A(2) + 6s_B(1)6s_B(2)) / \sqrt{2}$
$\Phi_3^s(r_1, r_2; R) = (\phi_3[\psi_3', \psi_3'] - \phi_4[\psi_4', \psi_4']) / \sqrt{2}$	$([6s_A, 6p_B] + [6s_B, 6p_A]) / \sqrt{2}$
$\Phi_4^s(r_1, r_2; R) = (\phi_3[\psi_3', \psi_3'] + \phi_4[\psi_4', \psi_4']) / \sqrt{2}$	$([6s_A, 6p_A] + [6s_B, 6p_B]) / \sqrt{2}$
$\Phi_1^u(r_1, r_2; R) = \phi_1[\psi_1', \psi_2']$	$(6s_A(1)6s_A(2) - 6s_B(1)6s_B(2)) / \sqrt{2}$
$\Phi_2^u(r_1, r_2; R) = (\phi_2[\psi_1', \psi_4'] - \phi_3[\psi_3', \psi_2']) / \sqrt{2}$	$([6s_B, 6p_A] - [6s_A, 6p_B]) / \sqrt{2}$
$\Phi_3^u(r_1, r_2; R) = (\phi_2[\psi_1', \psi_4'] + \phi_3[\psi_3', \psi_2']) / \sqrt{2}$	$([6s_A, 6p_A] - [6s_B, 6p_B]) / \sqrt{2}$

Table 4. Symmetrized combinations $\bar{\Phi}_j^{g,u}(r_1, r_2; R)$ of triplet one-configuration states $\bar{\phi}_i[\Psi_n, \Psi_n'] = [\Psi_n'(r_1)\Psi_n'(r_2) - \Psi_n'(r_2)\Psi_n'(r_1)]/\sqrt{2}$ and their atomic limits at $R \rightarrow \infty$

$\bar{\Phi}_j^{g,u}(r_1, r_2; R)$	Limit at $R \rightarrow \infty$ ($\bar{\chi}_j^{g,u}$)
$\bar{\Phi}_3^g(r_1, r_2; R) = (\bar{\phi}_3[\Psi_1', \Psi_3'] - \bar{\phi}_4[\Psi_2', \Psi_4'])/\sqrt{2}$	$([6s_A, 6p_B] + [6s_B, 6p_A])/\sqrt{2}$
$\bar{\Phi}_4^g(r_1, r_2; R) = (\bar{\phi}_3[\Psi_1', \Psi_3'] + \bar{\phi}_4[\Psi_2', \Psi_4'])/\sqrt{2}$	$([6s_A, 6p_A] + [6s_B, 6p_B])/\sqrt{2}$
$\bar{\Phi}_1^u(r_1, r_2; R) = \bar{\phi}_1[\Psi_1', \Psi_2']$	$[6s_B, 6s_A]$
$\bar{\Phi}_2^u(r_1, r_2; R) = (\bar{\phi}_2[\Psi_1', \Psi_4'] - \bar{\phi}_3[\Psi_3', \Psi_2'])/\sqrt{2}$	$([6s_A, 6p_A] - [6s_B, 6p_B])/\sqrt{2}$
$\bar{\Phi}_3^u(r_1, r_2; R) = (\bar{\phi}_2[\Psi_1', \Psi_4'] + \bar{\phi}_3[\Psi_3', \Psi_2'])/\sqrt{2}$	$([6s_B, 6p_A] - [6s_A, 6p_B])/\sqrt{2}$

singlet collisions, we have

$$\begin{aligned}
 \Psi_1(r_1, r_2; R) &= \Phi_1^g(r_1, r_2; R) \text{ (entrance channel),} \\
 \Psi_2(r_1, r_2; R) &= \frac{1}{\sqrt{2}}(\Phi_2^g(r_1, r_2; R) \\
 &+ \Phi_1^u(r_1, r_2; R)), (a) \quad 6s_A(1)6s_A(2); \\
 \Psi_3(r_1, r_2; R) &= \frac{1}{\sqrt{2}}(\Phi_2^g(r_1, r_2; R) \\
 &- \Phi_1^u(r_1, r_2; R)), (a') \quad 6s_B(1)6s_B(2); \quad (18) \\
 \Psi_4(r_1, r_2; R) &= \frac{1}{\sqrt{2}}(\Phi_3^g(r_1, r_2; R) \\
 &+ \Phi_2^u(r_1, r_2; R)), (c) \quad [6p_A, 6s_B]; \\
 \Psi_5(r_1, r_2; R) &= \frac{1}{\sqrt{2}}(\Phi_3^g(r_1, r_2; R) \\
 &- \Phi_2^u(r_1, r_2; R)), (c') \quad [6s_A, 6p_B].
 \end{aligned}$$

Here, $\Phi_j^{g,u}(r_1, r_2; R)$ are the two-electron states presented in Table 3. For triplet collisions, the following states were used:

$$\begin{aligned}
 \Psi_1(r_1, r_2; R) &= \bar{\Phi}_1^u(r_1, r_2; R) \text{ (entrance channel),} \\
 \Psi_2(r_1, r_2; R) &= \frac{1}{\sqrt{2}}(\bar{\Phi}_4^g(r_1, r_2; R) \\
 &+ \bar{\Phi}_2^u(r_1, r_2; R)), (b) \quad [6s_A, 6p_A], \\
 \Psi_3(r_1, r_2; R) &= \frac{1}{\sqrt{2}}(\bar{\Phi}_4^g(r_1, r_2; R) \\
 &- \bar{\Phi}_2^u(r_1, r_2; R)), (b') \quad [6s_B, 6p_B], \quad (19) \\
 \Psi_4(r_1, r_2; R) &= \frac{1}{\sqrt{2}}(\bar{\Phi}_3^g(r_1, r_2; R)
 \end{aligned}$$

$$\begin{aligned}
 &+ \bar{\Phi}_3^u(r_1, r_2; R)), (c) \quad [6s_B, 6p_A], \\
 \Psi_5(r_1, r_2; R) &= \frac{1}{\sqrt{2}}(\bar{\Phi}_3^g(r_1, r_2; R) \\
 &- \bar{\Phi}_3^u(r_1, r_2; R)), (c') \quad [6s_A, 6p_B].
 \end{aligned}$$

Here, $\bar{\Phi}_j^{g,u}(r_1, r_2; R)$ are the two-electron states presented in Table 4. Expressions (18) and (19) can be derived by using the limits of $\Phi_j^{g,u}$ and $\bar{\Phi}_j^{g,u}$ at $R \rightarrow \infty$ (see Tables 3 and 4).

To solve close-coupling equations (10), it is necessary to set initial conditions imposed on coefficients a_l .

At $t \rightarrow -\infty$ ($R \rightarrow \infty$), the quasi-molecule is in the state $\Psi_1(r_1, r_2) = \lim_{t \rightarrow -\infty} \Psi_1(r_1, r_2; R(t))$ with energy $E_1(\infty)$,

$$\tilde{\Psi}(r_1, r_2, t)|_{t \rightarrow -\infty} \rightarrow \Psi_1(r_1, r_2) \exp(-iE_1(\infty)t). \quad (20)$$

From (20) in view of expansion (8), we get initial conditions imposed on solutions to the close-coupling equations,

$$\begin{aligned}
 a_l(-\infty) &= \delta_{1l} \exp(-iv_1), \\
 v_1 &= \frac{1}{V} \int_0^\infty [E_1(R) - E_1(\infty)] \frac{R}{R - \gamma} d\tau. \quad (21)
 \end{aligned}$$

For given impact parameter ρ , the probability amplitude for transition from state $\Psi_1(r_1, r_2)$ to final state $\Psi_l(r_1, r_2) \approx \lim_{t \rightarrow \infty} \Psi_l(r_1, r_2; R(t))$ can be represented in the form

$$\begin{aligned}
 b_l(\rho, v) &= \lim_{t \rightarrow \infty} \langle \Psi_l(r_1, r_2) | \tilde{\Psi}(r_1, r_2, t) \rangle \exp(iE_l(\infty)t) \\
 &= a_l(v, \rho, \infty) \exp(-iv_l), \quad (22)
 \end{aligned}$$

where

$$v_l = \frac{1}{v} \int_0^{\infty} [E_l(R) - E_l(\infty)] \frac{R}{R - \gamma} d\tau.$$

Set (10) of close-coupling equations with initial conditions (21) was solved with the TANGO program [11]. At $R \leq R_0 = 30$ a.u., matrix elements $H_{ij}(R)$ of the two-electron Hamiltonian were calculated with the use of the program described in [10] (the matrix elements of the two-electron Hamiltonian calculated in bases (18) and (19) are given by relationships (15)). At $R > R_0$, energy $E_l(R)$ was calculated with the asymptotic expression

$$E_l(R) \approx E_l(\infty) - \frac{\alpha_l}{R} = E_l(R_0) - \alpha_l \left(\frac{1}{R} - \frac{1}{R_0} \right), \quad (23)$$

$\alpha_l = 8$ for $l = 1, 4, 5$ and $\alpha_l = 10$ for $l = 2, 3$.

The diagonal matrix elements for singlet states (18), $E_l(R) = H_{ll}(R)$, are shown in Fig. 1, where the dashed line is drawn for the energies of the two-electron states describing the channels of one-electron capture (b, b') into the triplet states of Bi^{3+} ions ($6s6p$). The energies of states $\Psi_{2,3}$ and $\Psi_{4,5}$ shown in Fig. 1 are shifted by -0.07 and -0.27 a.u. so that the resonance defects for channels (a, a'), (b, b'), and (c, c') coincide with the values obtained by atomic calculations.

At $R > R_0$, off-diagonal matrix elements $H_{lk}(R)$ of potential couplings were calculated by the extrapolation formulas

$$H_{lk}(R) = H_{lk}(R_0) \exp[-\beta_{lk}(R - R_0)]. \quad (24)$$

Coefficients β_{lk} entering into (24) were determined by the least-squares fit of the matrix elements of potential couplings obtained by (24) to the values calculated for nucleus spacing R varying between 12 and 30 a.u. The matrix elements of potential couplings for singlet collisions (1) are demonstrated in Fig. 2 (the dashed lines in the inset show $H_{lk}(R)$ calculated by formulas (24)).

The matrix elements of radial couplings between functions Ψ_l and Ψ_k , which enter into close-coupling equations (10), are expressed (up to terms quadratic in small parameters S_{13} and S_{24}) through the linear combinations of radial couplings $\langle 6s\sigma | d/dR | 7d\sigma \rangle$ and $\langle 7p\sigma | d/dR | 8f\sigma \rangle$ between single-electron SDMOs (13), which were calculated with the program package [10].

The nonzero matrix elements of radial couplings R_{lk}^1 and R_{lk}^3 between the singlet and triplet basic states are shown in Fig. 3.

Detailed calculations revealed that, for the collision energies we are interested in, the two-electron states are occupied mostly via potential interaction.

For given collision energy E_c , the cross sections of single-electron charge transfer, σ_{tr}^m , and excitation,

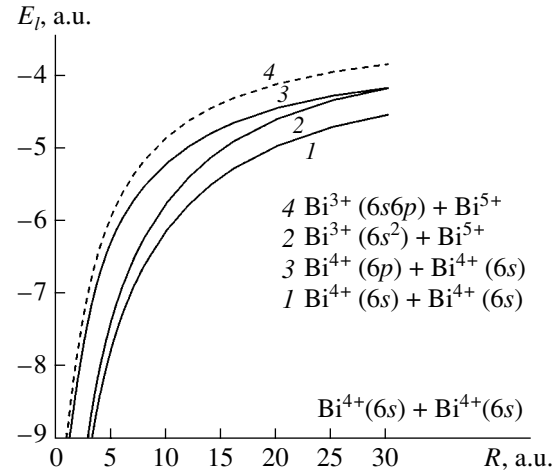


Fig. 1. Energies $E_l(R)$ of two-electron states $\Psi_l(r_1, r_2; R)$ for singlet $\text{Bi}^{4+}(6s) + \text{Bi}^{4+}(6s)$ collisions (reactions 1a, 1c) (on the right, the limits of Ψ_l at $R \rightarrow \infty$ are written): (1) entrance channel Ψ_1 , (2) charge transfer channels Ψ_2 and Ψ_3 (a, a'), (3) excitation channels Ψ_4 and Ψ_5 (c, c'), and (4) charge transfer channels Ψ_2 and Ψ_3 (b, b') in triplet collisions (reaction 1b).

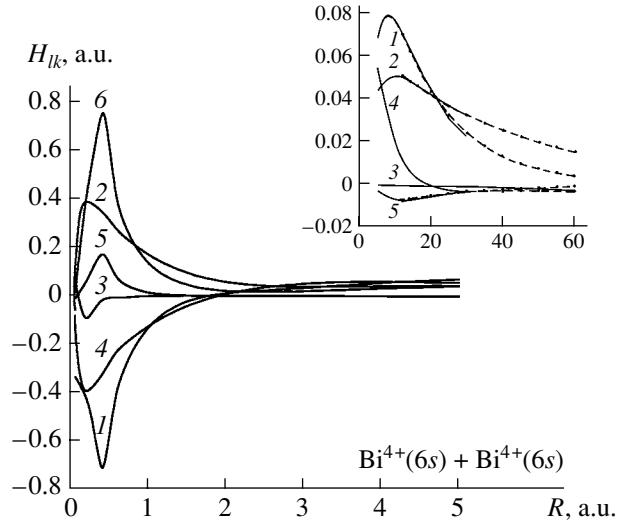


Fig. 2. Matrix elements of potential couplings H_{lk} between singlet states Ψ_l and Ψ_k : (1) $H_{12} = H_{13}$, (2) $H_{14} = H_{15}$, (3) $H_{23} = H_{25}$, (4) $H_{24} = H_{35}$, (5) $H_{25} = H_{34}$, and (6) $H_{45} = H_{34}$.

σ_{exc}^m , were calculated as

$$\sigma_{tr}^m(E_c) = 2\pi \int_0^{\infty} d\rho \rho |b_2^m(\rho, E_c)|^2, \quad (25)$$

$$\sigma_{exc}^m(E_c) = 2\pi \int_0^{\infty} d\rho \rho |b_4^m(\rho, E_c)|^2.$$

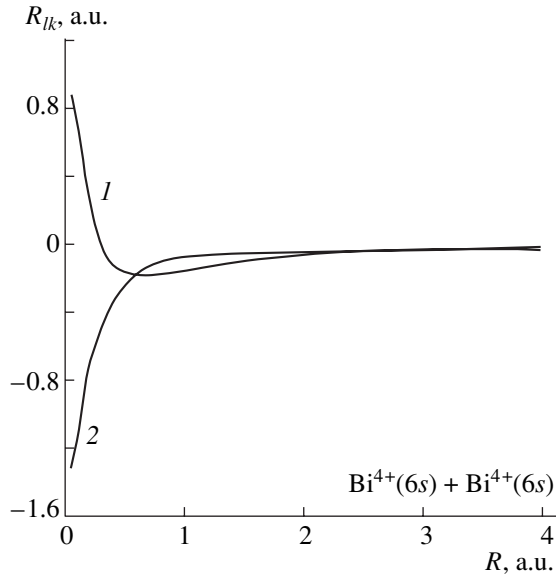


Fig. 3. Matrix elements of radial couplings R_{lk}^1 and R_{lk}^3 between singlet and triplet states Ψ_l and Ψ_k : (1) $R_{14}^1 = R_{15}^1 = R_{14}^3 = R_{51}^3$ and (2) $R_{24}^1 = R_{35}^1 = R_{21}^3 = R_{13}^3$.

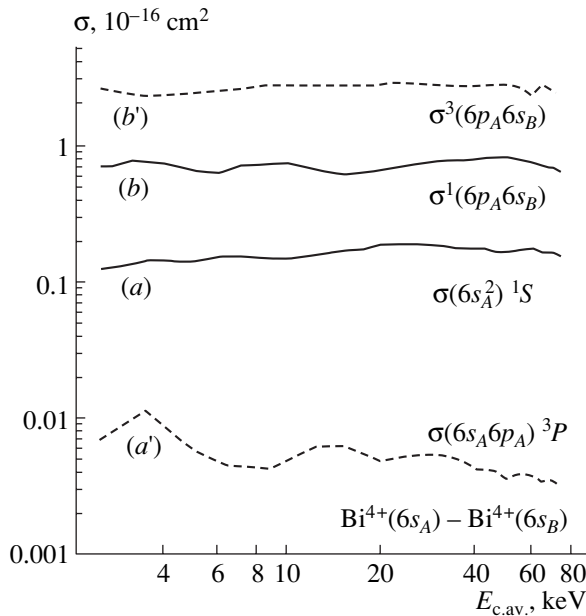


Fig. 4. Statistically weighted cross sections of charge transfer and excitation in $\text{Bi}^{4+}(6s)\text{-Bi}^{4+}(6s)$ collisions: cross sections $\sigma(6s_A^2)^1S$ and $\sigma(6s_A 6p_A)^3P$ of charge transfer into (a) $\text{Bi}^{3+}(6s^2)$ singlet and (a') $\text{Bi}^{3+}(6s6p)$ triplet states of the ions, respectively, and the cross sections of the $6s_A \rightarrow 6p_A$ excitation of the incident ion for the (b) singlet, $\sigma^1(6p_A 6s_B)$, and (b') triplet, $\sigma^3(6p_A 6s_B)$, entrance channels.

Here, $b_2^m(\rho, E_c)$ and $b_4^m(\rho, E_c)$ are the probability amplitudes (see (22)) for transition from initial state $\Psi_1(r_1, r_2)$ to final states $\Psi_2(r_1, r_2)$ and $\Psi_4(r_1, r_2)$ obtained by solving close-coupling equations (10) written in the basis of singlet ($m = 1$) and triplet ($m = 3$) quasi-molecular states. For the probability amplitudes calculated, the relationships $b_2^m(\rho, E_c) = b_3^m(\rho, E_c)$ and $b_4^m(\rho, E_c) = b_5^m(\rho, E_c)$ are valid.

The total cross sections of single-electron charge transfer, Σ_{tr} , and single-electron excitation of an incident ion, Σ_{exc} , were calculated as a sum of the statistically weighted charge-transfer and excitation cross sections calculated for the singlet and triplet channels,

$$\Sigma_{\text{tr}} = \sigma(6s_A^2)^1S + \sigma(6s_A 6p_A)^3P \equiv 0.25\sigma_{\text{tr}}^1 + 0.75\sigma_{\text{tr}}^3,$$

$$\begin{aligned} \Sigma_{\text{exc}} &= \sigma^1(6p_A 6s_B) + \sigma^3(6p_A 6s_B) \\ &\equiv 0.25\sigma_{\text{exc}}^1 + 0.75\sigma_{\text{exc}}^3. \end{aligned}$$

The calculated sections (Fig. 4) depend on the collision energy only slightly. The cross sections of charge transfer into the singlet, $6s^2$, and triplet, $6s6p$, states of Bi^{3+} ions vary in the ranges $(1.2\text{--}1.9) \times 10^{-17}$ and $(0.3\text{--}1.0) \times 10^{-18}$ cm^2 , respectively; cross sections $\sigma^1(6p_A 6s_B)$ and $\sigma^3(6p_A 6s_B)$, in the ranges $(0.6\text{--}0.8) \times 10^{-16}$ and $(2.2\text{--}2.8) \times 10^{-16}$ cm^2 , respectively. The process of charge transfer into the $\text{Bi}^{3+}(6s^2)$ state is a major contributor to total cross section Σ_{tr} of single-electron charge transfer in $\text{Bi}^{4+}(6s)\text{-Bi}^{4+}(6s)$ collisions.

CROSS SECTIONS OF SINGLE-ELECTRON AND RESONANCE CHARGE TRANSFER IN $\text{Bi}^{4+}(6s)\text{-Bi}^{4+}(6p)$ COLLISIONS

Collision between two Bi^{4+} ions, one in the ground and the other in the metastable state, was calculated for the singlet and triplet entrance channels in the basis of six (three even and three odd) two-electron states $\Phi_j^{g,u}(r_1, r_2; R)$ taken from Table 3,

$$\Psi_1^g = \Phi_3^g, \quad \Psi_2^g = \Phi_2^g, \quad \Psi_3^g = \Phi_4^g, \quad (26)$$

$$\text{and } \Psi_1^u = \Phi_2^u, \quad \Psi_2^u = \Phi_1^u, \quad \Psi_3^u = \Phi_3^u$$

and in the basis of four (two even and two odd) two-electron states $\bar{\Phi}_j^{g,u}(r_1, r_2; R)$ taken from Table 4,

$$\bar{\Psi}_1^g = \bar{\Phi}_3^g, \quad \bar{\Psi}_2^g = \bar{\Phi}_4^g \quad \text{and} \quad \bar{\Psi}_1^u = \bar{\Phi}_3^u, \quad \bar{\Psi}_2^u = \bar{\Phi}_2^u. \quad (27)$$

To solve close-coupling equations (10) in the basis of singlet, (26), and triplet, (27), states, it is necessary to set initial conditions imposed to coefficients $a_j^{g,u}$ multiplying even and odd basic functions in expansion (8).

Table 5. Wave functions Ψ_k describing the final states of the system in singlet collisions (2) and the probability amplitudes for transition to these states

Z_A	Z_B	(k)	Ψ_k	b_k^1
$\text{Bi}^{3+}(6s6p) + \text{Bi}^{5+}$		(a)	$\frac{1}{\sqrt{2}}(\chi_3^g + \chi_3^u)$	$b_a^1 = 0.5(T_3^g + T_3^u)$
$\text{Bi}^{5+} + \text{Bi}^{3+}(6s6p)$		(a')	$\frac{1}{\sqrt{2}}(\chi_3^g - \chi_3^u)$	$b_{a'}^1 = 0.5(T_3^g - T_3^u)$
$\text{Bi}^{3+}(6s^2) + \text{Bi}^{5+}$		(b)	$\frac{1}{\sqrt{2}}(\chi_2^g + \chi_2^u)$	$b_b^1 = 0.5(T_2^g + T_2^u)$
$\text{Bi}^{5+} + \text{Bi}^{3+}(6s^2)$		(b')	$\frac{1}{\sqrt{2}}(\chi_2^g - \chi_2^u)$	$b_{b'}^1 = 0.5(T_2^g - T_2^u)$
$\text{Bi}^{4+}(6p) + \text{Bi}^{4+}(6s)$		(c)	$\frac{1}{\sqrt{2}}(\chi_1^g + \chi_1^u)$	$b_c^1 = 0.5(T_1^g + T_1^u)$

At the zero time, $t \rightarrow -\infty$ ($R \rightarrow \infty$), the quasi-molecule is in state $\Psi_1(r_1, r_2)$ with energy \tilde{E}_1 ,

$$\tilde{\Psi}(r_1, r_2, t)|_{t \rightarrow -\infty} \rightarrow \Psi_1(r_1, r_2) \exp(-i\tilde{E}_1 t). \quad (28)$$

In the collisions of interest, function $\Psi_1(r_1, r_2)$ describes the state of the system when one electron is near nucleus Z_A in state $6s$ and the other is near nucleus Z_B in state $6p$. Using atomic limits (17) of functions $\Phi_j^{g,u}(r_1, r_2; R)$ and $\bar{\Phi}_j^{g,u}$ listed in Tables 3 and 4, we find that function $\Psi_1(r_1, r_2)$ for singlet and triplet collisions (2) has the form

$$\Psi_1(r_1, r_2) = \begin{cases} (\chi_1^g - \chi_1^u)/\sqrt{2} \\ (\bar{\chi}_1^g - \bar{\chi}_1^u)/\sqrt{2}. \end{cases} \quad (29)$$

Substituting expressions (8) and (29) into (28), we find that, at $t \rightarrow -\infty$,

$$a_j^{g,u}(-\infty) = \begin{cases} \delta_{1j} \exp(-i v_1^{g,u})/\sqrt{2} \\ \delta_{1j} \exp(-i \bar{v}_1^{g,u})/\sqrt{2} \end{cases} \quad (30)$$

with regard to the orthogonality of functions $\chi_j^{g,u}$ and $\bar{\chi}_j^{g,u}$.

For the singlet channel, phases $v_1^{g,u}$ have the form

$$v_1^{g,u} = \int_0^\infty (E_1^{g,u}(R) - \tilde{E}_1) \frac{R}{R - \gamma} d\tau,$$

where $\tilde{E}_1 = \lim_{R \rightarrow \infty} E_1^{g,u}(R)$ and $E_1^{g,u}(R)$ are the matrix elements of $\langle \Psi_1^{g,u} | H | \Psi_1^{g,u} \rangle$. For the triplet channel, the respective expressions are similar.

The even and odd states of a homonuclear quasi-molecule are not coupled, since the electron coordinate system is placed in the middle of the nuclear spacing, and so set (10) of close-coupling equations splits into two independent sets of ordinary differential equations in coefficients a_j^g and a_j^u with initial conditions (30). Coefficients c_j appearing in initial conditions

$$c_j(-\infty) = \delta_{1j} \exp\left(-\frac{i}{v} v_1\right)$$

to the set of close-coupling equations are found using the TANGO program package [11]. From the linearity of the close-coupling equations, it follows that

$$a_j^{g,u}(\tau) = \frac{1}{\sqrt{2}} c_j^{g,u}(\tau). \quad (31)$$

Using the limits of functions $\Phi_j^{g,u}$ and $\bar{\Phi}_j^{g,u}$ at $R \rightarrow \infty$ (Tables 3 and 4), we can find wave functions $\Psi_k(r_1, r_2)$ (see Tables 5 and 6) that describe the states of the system at $t \rightarrow \infty$ corresponding to the singlet and triplet channels $k = (1a)-(1c)$ in $\text{Bi}^{4+}(6s) + \text{Bi}^{4+}(6p)$ collisions,

$$\Psi_k(r_1, r_2) = \begin{cases} \lambda_k^g \chi_i^g + \lambda_k^u \chi_i^u, & i = 1-3 \\ \bar{\lambda}_k^g \bar{\chi}_j^g + \bar{\lambda}_k^u \bar{\chi}_j^u, & i = 1, 2. \end{cases} \quad (32)$$

With regard to relationships (31) and (32), the probability amplitude for transition from state $\Psi_1(r_1, r_2)$ to final state $\Psi_k(r_1, r_2)$ with energy \tilde{E}_k ,

$$b_k = \lim \langle \Psi_k(r_1, r_2) | \tilde{\Psi}(r_1, r_2, t) \rangle \exp(i\tilde{E}_k t) |_{t \rightarrow \infty}$$

is expressed through calculated quantities $c_j^{g,u}$ as fol-

Table 6. Wave functions Ψ_k describing the final states of the system in triplet collisions (2) and the probability amplitudes for transition to these states

Z_A	Z_B	(k)	Ψ_k	b_k^3
$\text{Bi}^{3+}(6s6p) + \text{Bi}^{5+}$		(a)	$\frac{1}{\sqrt{2}}(\bar{\chi}_2^g + \bar{\chi}_2^u)$	$b_a^3 = 0.5(\bar{T}_2^g + \bar{T}_2^u)$
$\text{Bi}^{5+} + \text{Bi}^{3+}(6s6p)$		(a')	$\frac{1}{\sqrt{2}}(\bar{\chi}_2^g - \bar{\chi}_2^u)$	$b_{a'}^3 = 0.5(\bar{T}_2^g - \bar{T}_2^u)$
$\text{Bi}^{4+}(6p) + \text{Bi}^{4+}(6s)$		(c)	$\frac{1}{\sqrt{2}}(\bar{\chi}_1^g + \bar{\chi}_1^u)$	$b_c^3 = 0.5(\bar{T}_1^g + \bar{T}_1^u)$

lows:

$$b_k^m(\rho, E_c) = \begin{cases} (\lambda_k^g T_i^g + \lambda_k^u T_i^u) / \sqrt{2} \\ (\bar{\lambda}_k^g \bar{T}_j^g + \bar{\lambda}_k^u \bar{T}_j^u) / \sqrt{2}, \end{cases} \quad (33)$$

where

$$T_i^{g,u} = c_i^{g,u}(\infty) \exp(-i\nu_i^{g,u}),$$

$$\bar{T}_j^{g,u} = \bar{c}_j^{g,u}(\infty) \exp(-i\bar{\nu}_j^{g,u})$$

and $c_i^{g,u}$ and $\bar{c}_j^{g,u}$ are the solutions to the set of close-coupling equations written in the basis of singlet, (26), and triplet, (27), states. For the singlet channel, phases

$\nu_i^{g,u}$ have the form

$$\nu_i^{g,u} = \frac{1}{v} \int_0^\infty [E_i^{g,u}(R) - \tilde{E}_k] \frac{R}{R-\gamma} d\tau,$$

where $\tilde{E}_k = \lim_{R \rightarrow \infty} E_i^{g,u}(R)$ and $E_i^{g,u}(R)$ are the matrix elements of $\langle \Psi_i^{g,u} | H | \Psi_i^{g,u} \rangle$. For the triplet channel, the respective expressions are similar.

The partial cross sections of occupation of the final singlet ($m=1$) and triplet ($m=3$) states in reactions (2) were calculated by the formulas

$$\sigma_k^m(E_c) = 2\pi \int_0^\infty d\rho \rho |b_k^m(\rho, E_c)|^2.$$

The computational formulas for transition probability amplitudes b_k^m are given in Tables 5 and 6.

The matrix elements of potential and radial couplings between bases (26) and (27), which enter into the close-coupling equations, were calculated with the program package described in [10]. Diagonal matrix elements $E_j^{g,u}(R)$ of two-electron Hamiltonian that were calculated for the singlet set of basic states (26) are shown in Fig. 5.

Figure 6 demonstrates the statistically weighted partial cross sections of single-electron charge transfer into the singlet (channels a and a' in Table 5) and triplet (channels a , a' in Table 6) states of $\text{Bi}^{3+}(6s6p)$ ions,

$$\sigma(6s_A 6p_A)^1 P = 0.25 \sigma_a^1, \quad \sigma(6s_B 6p_B)^1 P = 0.25 \sigma_{a'}^1, \quad (34)$$

$$\sigma(6s_A 6p_A)^3 P = 0.75 \sigma_a^3, \quad \sigma(6s_B 6p_B)^3 P = 0.75 \sigma_{a'}^3, \quad (35)$$

and also the cross sections of resonance charge transfer for the singlet and triplet entrance channels,

$$\sigma(6p_A 6s_B)^1 P = 0.25 \sigma_c^1, \quad \sigma(6p_A 6s_B)^3 P = 0.25 \sigma_c^3 \quad (36)$$

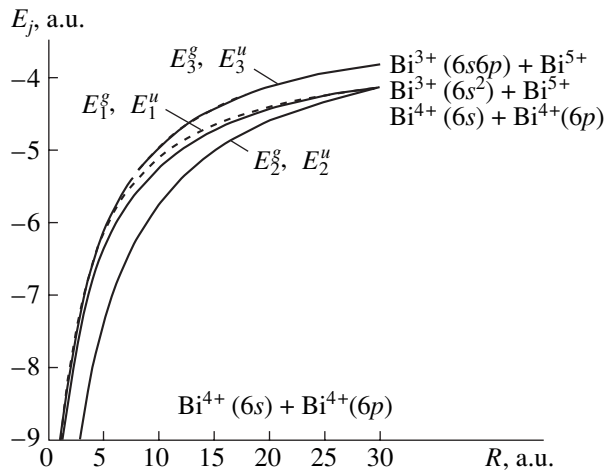


Fig. 5. Diagonal matrix elements $E_j^{g,u}(R)$ of the two-electron Hamiltonian that were calculated in the basis of singlet states $\Psi_j^{g,u}(r_1, r_2; R)$ for the g (continuous lines) and u (dashed line) symmetry (the energies of states Ψ_2^g , Ψ_2^u and Ψ_3^g , Ψ_3^u are indistinguishable on the plot). On the right, the limits of Ψ_j at $R \rightarrow \infty$ are written.

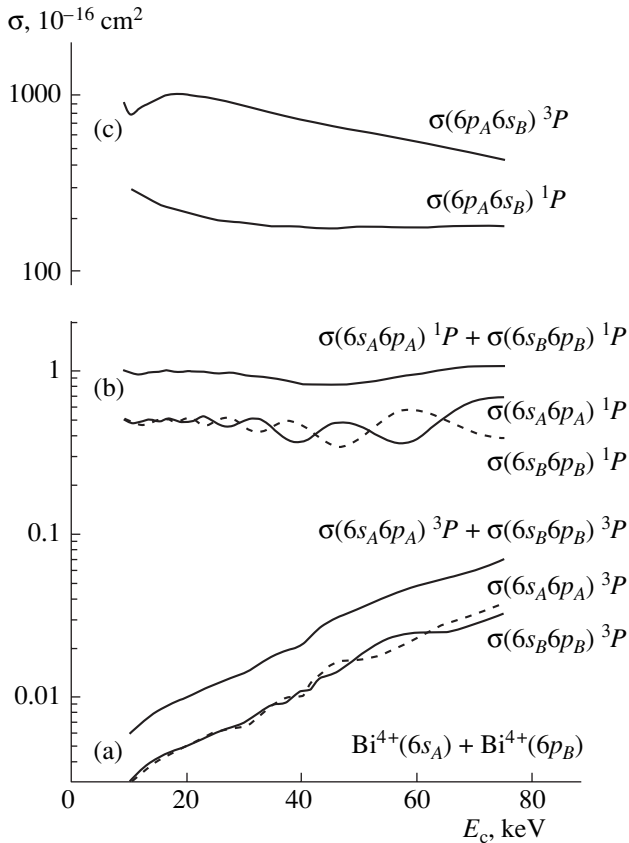


Fig. 6. Statistically weighted cross sections of single-electron and resonance charge transfer in $\text{Bi}^{4+}(6s)\text{-Bi}^{4+}(6p)$ collisions (reactions 2): (a) partial, $\sigma(6s_A 6p_A)^{3P}$ and $\sigma(6s_B 6p_B)^{3P}$, and total cross sections of single-electron charge transfer into the triplet $\text{Bi}^{3+}(6s6p)$ states (channels a and a' , Table 6); (b) partial, $\sigma(6s_A 6p_A)^{1P}$ and $\sigma(6s_B 6p_B)^{1P}$, and total cross sections of single-electron charge transfer into the singlet $\text{Bi}^{3+}(6s6p)$ states (channels a and a' , Table 5); and (c) cross sections of resonance charge transfer, $\sigma(6p_A 6s_B)^{1P}$ and $\sigma(6p_A 6s_B)^{3P}$, for the singlet (channel c , Table 5) and triplet (channel c , Table 6) entrance channels.

(the partial cross sections of single-electron capture into the $\text{Bi}^{3+}(6s^2)$ states, σ_b^1 and $\sigma_{b'}^1$, are three orders of magnitude smaller than σ_a^1 and $\sigma_{a'}^1$ and are therefore omitted in Fig. 6). It follows from Fig. 6 that, for both the singlet and triplet entrance channels, the partial cross sections of occupation of the $6s6p$ states in the incident ion, $\sigma(6s_A 6p_A)$, and in the target ion, $\sigma(6s_B 6p_B)$, differ insignificantly at low collision energies. As the energy grows, the respective curves diverge, oscillating in antiphase. The sum of the cross sections of single-electron capture into the $\text{Bi}^{3+}6s6p$ singlet states depends on the collision energy only slightly, while for the triplet states, it grows with energy, remaining smaller than the cross section of single-electron capture into the singlet states by one order of magnitude.

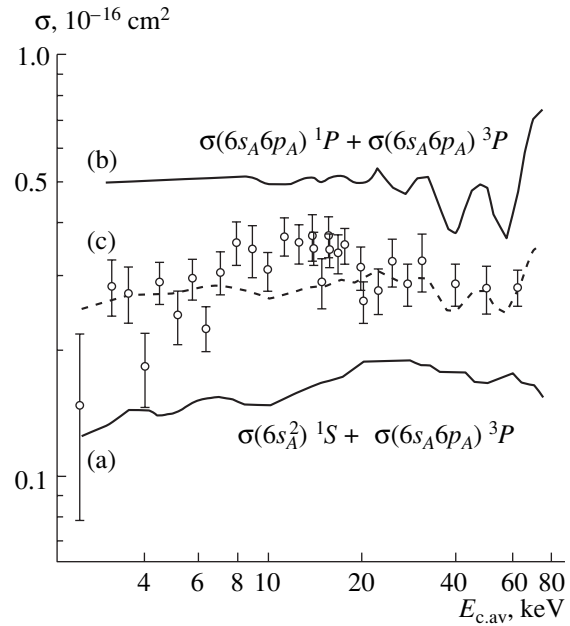


Fig. 7. Charge transfer total cross sections in (a) $\text{Bi}^{4+}(6s)\text{-Bi}^{4+}(6s)$ and (b) $\text{Bi}^{4+}(6s)\text{-Bi}^{4+}(6p)$ collisions and (c) the weighted average charge transfer cross section for fractions of reactions 1 and 2 of 0.59 and 0.41, respectively. (c) Charge transfer total cross section obtained in crossed-beam experiments [2].

The total cross section of single-electron charge transfer in $\text{Bi}^{3+}(6s) + \text{Bi}^{4+}(6p)$ collisions, Σ_{tr} , was calculated as a sum of the statistically weighted cross sections of single-electron charge transfer for the singlet, (34), and triplet, (35), entrance channels,

$$\Sigma_{\text{tr}} = \sigma(6s_A 6p_A)^{1P} + \sigma(6s_A 6p_A)^{3P}.$$

Figure 7 compares the charge transfer total cross sections calculated for two ground-state Bi^{4+} ions (reactions 1) and for two Bi^{4+} ions one of which is in the ground and the other in the excited (metastable) state (reactions 2) with experimental data [2]. The dependences of the charge transfer cross sections on the collision energy are in qualitative agreement with the data points; however, the absolute values of the charge transfer cross sections for $\text{Bi}^{4+}(6s)\text{-Bi}^{4+}(6s)$ collisions (reactions 1) are roughly twice as low as the experimental data. The charge transfer total cross section for $\text{Bi}^{4+}(6s)\text{-Bi}^{4+}(6p)$ collisions (reactions 2) is, as expected, higher than the charge transfer total cross section for collisions between the ground-state ions.

The dashed line in Fig. 7 refers to the charge transfer total cross section in the case when the fractions of reactions 1 and 2 are 0.59 and 0.41, respectively (such values of the fractions were selected by comparing the total theoretical cross section with the sum of the experimental cross sections for all data points in Fig. 7). Such

a proportion implies that the fraction of metastable ions amounts to 20% in either of crossed beams.

CONCLUSIONS

The cross sections of single-electron charge transfer and $6s \rightarrow 6p$ electronic excitation in collisions between ground-state $\text{Bi}^{4+}(6s)$ ions and the cross sections of charge transfer in collisions between Bi^{4+} ions in the ground ($6s$) and metastable ($6p$) states were calculated by solving close-coupling equations written in the basis of two-electron quasi-molecular states.

For the triplet reaction channel, the cross section of $6s \rightarrow 6p$ excitation for a ground-state $\text{Bi}^{4+}(6s)$ ion colliding with another ground-state $\text{Bi}^{4+}(6s)$ ion is roughly three times as large as that for the singlet reaction channel.

The dependence of the charge transfer cross sections on the orientation of the electron spins of colliding ions was studied. For the collision energy interval 5–75 keV in the center-of-mass coordinate system (the relative velocity of colliding ions is ~ 0.1 a.u.), the processes of single-electron charge transfer into the singlet $\text{Bi}^{3+}(6s^2)$ states (reactions 1) and into the singlet $\text{Bi}^{3+}(6s6p)$ states (reactions 2) dominate in $\text{Bi}^{4+}(6s)\text{--}\text{Bi}^{4+}(6s)$ collisions (reactions 1) and in $\text{Bi}^{4+}(6s)\text{--}\text{Bi}^{4+}(6p)$ collisions (reactions 2), respectively. The cross section of charge transfer in reactions 2 is roughly three times as large as that in reactions 1.

Reliable data for charge transfer and electronic excitations in collisions between heavy four-charged bismuth ions in the kiloelectronvolt range of collision energies are obtained for the first time. As was noted in [2], theoretical results for such collisions [12] disagree with experimental data even qualitatively. The results reported in [12] were obtained in the Oppenheimer–Brinkman–Kramers approximation, with (importantly!) the $\text{Bi}^{4+}\text{--}\text{Bi}^{4+}$ two-electron quasi-molecule considered as a system with one active electron, which was described in terms of hydrogen-like wave functions with bare effective charges of the projectile and target.

The data for the charge transfer cross sections obtained in this work may be useful, specifically, for

estimating particle losses in relativistic ion beams due to a change in the charge state of the ions colliding with each other in the beam because of its betatron oscillations.

ACKNOWLEDGMENTS

The authors are indebted to the International Atomic Energy Agency for financial support, contract no. 13348/RBF.

We thank A. Salin and R. Trassl for assistance.

REFERENCES

1. I. Hofmann, Nucl. Instrum. Methods Phys. Res. A **464**, 24 (2001).
2. A. Diehl, H. Brauning, R. Trassl, et al., J. Phys. B **34**, 4073 (2001).
3. V. K. Nikulin and N. A. Guschina, in *Proceedings of the 23rd International Conference on Photonic, Electronic and Atomic Collisions (ICPEAC), Stockholm, 2003*, p. Tu165.
4. V. K. Nikulin and N. A. Guschina, J. Phys. B **11**, 3553 (1978).
5. I. V. Komarov, L. I. Ponomarev, and S. Yu. Slavyanov, *Spheroidal and Coulomb Spheroidal Functions* (Nauka, Moscow, 1976), p. 171.
6. M. Barat and W. Lichten, Phys. Rev. A **6**, 221 (1972).
7. V. K. Nikulin and N. A. Gushchina, Opt. Spektrosk. **80**, 378 (1996) [Opt. Spectrosc. **80**, 333 (1996)].
8. N. A. Gushchina, V. K. Nikulin, A. V. Samoilov, et al., Preprint No. 811, FTI (Physicotechnical Institute im. A.F. Ioffe, Leningrad, 1983).
9. P. O. Löwdin, J. Chem. Phys. **18**, 365 (1950).
10. N. A. Gushchina and V. K. Nikulin, Preprint No. 1717, FTI (Ioffe Physicotechnical Institute, Russian Academy of Sciences, St. Petersburg, 1998).
11. R. D. Piacentini and A. Salin, Comput. Phys. Commun. **12**, 199 (1976).
12. V. P. Shevel'ko, Zh. Tekh. Fiz. **71** (10), 20 (2001) [Tech. Phys. **46**, 1225 (2001)].

Translated by V. Isaakyan